Quarterly Journal of the Royal Meteorological Society Q. J. R. Meteorol. Soc. 143: 1148–1164, January 2017 B DOI:10.1002/qj.3001

Royal Meteorological Society

The connection between extreme stratospheric polar vortex events and tropospheric blockings

Jinlong Huang, Wenshou Tian,* Jiankai Zhang, Qian Huang, Hongying Tian and Jiali Luo
Key Laboratory for Semi-Arid Climate Change of the Ministry of Education, College of Atmospheric Sciences, Lanzhou University, China

*Correspondence to: W. Tian, Key Laboratory for Semi-Arid Climate Change of the Ministry of Education, College of Atmospheric Sciences, Lanzhou University, Lanzhou 730000, China. E-mail: wstian@lzu.edu.cn

The variations of tropospheric blockings and their connections with the stratospheric polar vortex during different stages of the life cycle of extreme stratospheric polar vortex events (i.e. strong vortex (SV) events and weak vortex (WV) events) are investigated. The blocking frequency decreases over the Euro-Atlantic sector and increases over the western North Pacific during the onset and maturation stages of SV events. There are more blocking days over the western North Pacific and weakened upward planetary wave fluxes in the stratosphere during the maturation stage of shorter time-scale SV events than during longer time-scale SV events and the weakening of the upward planetary wave fluxes mainly results from the linear wave interference effect. The blocking frequency is increased over the Euro-Atlantic sector during the decline stage of SV events. This increase is found to be related to the descending stratospheric zonal wind anomalies and the poleward displacement of the eddy-driven jet stream, which lasts for about 10 days and is associated with the descending positive stratospheric Northern Annular Mode (NAM) anomalies. The increased blocking frequency leads to an enhancement of the planetary wave fluxes in the stratosphere via both the linear wave interference (for shorter time-scale SV events) and nonlinear wave interference (for longer time-scale SV events) effect.

The changes of the blocking frequency during the growth stage of WV events are almost opposite to those observed during the onset and maturation stages of SV events. The blocking frequency decreases over the Euro-Atlantic sector after the central dates of WV events, which are related to the descending stratospheric zonal wind anomalies and the equatorward displacement of the eddy-driven jet stream preceded by the descending negative stratospheric NAM anomalies about 10 days. We found that the nonlinear wave interference begins to make a considerable contribution to the weakening of the upward wave fluxes in the stratosphere after the central date of WV events and this is not emphasized in previous literature.

Key Words: stratospheric polar vortex; tropospheric blockings; planetary waves; wave interference; Northern Annular Mode

Received 24 June 2016; Revised 2 January 2017; Accepted 15 January 2017; Published online in Wiley Online Library

1. Introduction

The dynamical linkage between the stratospheric polar vortex and tropospheric blockings is a debated topic that has been widely discussed for many years. Several authors have demonstrated an interaction between the stratospheric polar vortex and tropospheric blockings (Quiroz, 1986; Mukougawa *et al.*, 2005; Kuroda, 2008; Martius *et al.*, 2009; Castanheira and Barriopedro, 2010; Nishii *et al.*, 2010, 2011; Woollings *et al.*, 2010; Vial *et al.*, 2013; Davini *et al.*, 2014a). However, it is not easy to determine an obvious connection between the stratospheric polar vortex and tropospheric blockings. Taguchi (2008) used a random shuffling method to examine possible connections between major stratospheric sudden warming (SSW) and tropospheric blocking events and he found no evident variations in preference of blocking events in the pre-SSW period and in the occurrence and duration of blocking events in the post-SSW period. Part of the less obvious relationship between them is due to strong variability in blocking activity during extreme stratospheric polar vortex events. Thus, it is worthwhile to re-examine the connection between the stratospheric polar vortex and tropospheric blockings in more detail.

The stratospheric polar vortex, which is a belt of strong circumpolar westerly winds over the polar region, plays a critical role in the dynamical coupling between the stratosphere and troposphere (Hartley *et al.*, 1998; Baldwin and Dunkerton, 1999, 2001; Thompson *et al.*, 2002; Black, 2002; Black and McDaniel, 2004; Limpasuvan *et al.*, 2004, 2005; Charlton and Polvani, 2007; Kolstad *et al.*, 2010; Mitchell *et al.*, 2013; Xie *et al.*, 2016; Zhang *et al.*, 2016). Significant stratospheric anomalies in the polar stratosphere (e.g. temperature anomalies, zonal wind anomalies) are often followed by corresponding tropospheric anomalies and there are significant variations in the upward propagation of planetary waves from the troposphere when the wind strength and wind direction of the stratospheric polar vortex undergo strong variations (Andrews *et al.*, 1987; Baldwin and Dunkerton, 2001; Polvani and Kushner, 2002; Wang and Chen, 2010; Hitchcock and Simpson, 2014). Strong variations in the stratospheric polar vortex are usually referred to as extreme stratospheric polar vortex events, which can be divided into two types based on the index of the Northern Annular Mode (NAM) or Arctic Oscillation (AO) (Thompson and Wallace, 1998; Baldwin and Dunkerton, 2001) or the zonal-mean zonal wind (Limpasuvan *et al.*, 2004), polar cap geopotential height anomalies (Kolstad *et al.*, 2010), polar cap temperature anomalies (Nakagawa and Yamazaki, 2006) and so on. The weak vortex and strong vortex (WV and SV) events can be determined based on the anomalous values in the aforementioned variables, most commonly, negative values of NAM or AO correspond to WV events, and positive values correspond to SV events (Baldwin and Dunkerton, 2001). WV events are characterized by a weakening of the polar vortex, with a warming stratospheric temperature and an increase in geopotential height over the polar region, vice versa for SV events (Limpasuvan *et al.*, 2004, 2005; Kuroda, 2008). Some WV events are also referred to as SSW events (Matsuno, 1971) in which the 10 hPa zonal-mean westerlies at 60°N undergo a reversal, followed by a remarkable increase in the polar stratospheric temperature over a short period of time (Mcintyre, 1982). WV and SV events are associated with variations in upward fluxes of planetary waves consisting primarily of zonal wave-numbers 1 and 2 from the troposphere (Charney and Drazin, 1961; Matsuno, 1971; Perlwitz and Graf, 2001; Limpasuvan *et al.*, 2004, 2005; Chen *et al.*, 2005).

Many previous studies have noted that the anomalous upward fluxes of planetary waves from the troposphere to the stratosphere are closely related to tropospheric blockings (Quiroz, 1986; Mukougawa and Hirooka, 2004; Kuroda, 2008; Martius *et al.*, 2009; Castanheira and Barriopedro, 2010; Nishii *et al.*, 2010, 2011; Woollings *et al.*, 2010; Vial *et al.*, 2013; Ayarzaguena *et al.*, 2015). On the other hand, Marshall and Scaife (2010) found that the predictability of stratospheric warmings and Atlantic blocking signatures can be improved when the stratosphere was better represented in a numerical model, implying a role of the stratosphere in the evolution of tropospheric blockings. In addition, the geographic location of tropospheric blockings is important in the occurrence of WV and SV events because the influence of tropospheric blockings on the upward fluxes of planetary waves exhibits regional differences. For instance, Martius *et al.* (2009) showed that the blocking tends to be detected over the Atlantic basin and enhances the upward fluxes of planetary waves before SSW events. Castanheira and Barriopedro (2010) detected an enhancement of the amplitude of planetary wave-1 at 100 hPa during Euro-Atlantic blocking events accompanied by a decrease in NAM index at 50 hPa and an enhancement of the amplitude of planetary wave-2 at 100 hPa during Pacific blocking events accompanied by an increase in NAM index at 50 hPa. Nishii *et al.* (2011) revealed the influence of the Euro-Atlantic blocking events and western Pacific blocking events on the upward fluxes of planetary waves by applying the linear interference between climatological and anomalous planetary waves related to blocking. The linear wave interference includes the reduced or enhanced amplitude of planetary waves due to the anti-phase or in-phase superposition of climatological and anomalous waves. Many of the abovementioned studies analysed the effects of tropospheric blockings on planetary waves prior to WV or SV events based on composites of blocking events. However, the details of the evolution of tropospheric blockings during different stages of the life cycle of WV and SV events remain unclear. In addition, the mechanisms through which tropospheric blockings affect the stratospheric polar vortex during different stages of the life cycle of WV and SV events are also not fully understood.

Conversely, WV and SV events may also influence tropospheric blockings at a later stage, which has been established by some authors (i.e. Woollings *et al.*, 2010; Kodera *et al.*, 2013; Lu and Ding, 2013; Vial *et al.*, 2013; Davini *et al.*, 2014a). Several mechanisms have been proposed to explain how WV and SV events affect tropospheric blockings, for example, by modulating the tropospheric eddy-driven jet displacements (Davini *et al.*, 2014a), by affecting the North Atlantic Oscillation (NAO) (e.g. Shabbar *et al.*, 2001; Barriopedro *et al.*, 2006; Croci-Maspoli *et al.*, 2007; Vial *et al.*, 2013), and by reflecting the upward propagating planetary waves following the weakening of the stratospheric polar vortex (Kodera *et al.*, 2013). Some other studies found that the upward fluxes of planetary waves are weakened and enhanced during the later stage of WV and SV events, respectively (Limpasuvan *et al.*, 2004, 2005; Kuroda, 2008). It is apparent from these abovementioned studies that there is an interaction between extreme stratospheric polar vortex events and tropospheric blockings. However, the coupling mechanisms between them are not straightforward and some questions remain, e.g. is it possible that the tropospheric blockings that are altered due to descending anomalies from the stratosphere affect the variation in the upward fluxes of planetary waves during the later periods of WV and SV events? If so, are the vertical wave activity flux anomalies in the later periods of the two types of events still dominated by the linear interference between climatological and anomalous waves related to the blockings?

In this study, we attempt to show more details of the evolution of the tropospheric blockings at each stage of WV and SV events. We also attempt to clarify the role of wave interference effects in the process of the dynamical coupling between the tropospheric blockings and the stratospheric polar vortex in different stages of the life cycle of WV and SV events. This article is structured as follows: section 2 presents the data and methodology; sections 3–5 present the main results; and section 6 provides a summary of this work.

2. Data and methods

The National Centers for Environmental Prediction/National Center for Atmospheric Research (NCEP/NCAR) reanalysis dataset is used in this study. The dataset has a horizontal resolution of $2.5^\circ \times 2.5^\circ$ and 17 pressure levels from 1000 to 10 hPa. Sixty-five extended winters (November to March) are analysed from 1948 to 2013. The anomalies presented in this study are computed as deviations from the daily climatological annual cycle. A 31-day running-mean is performed on daily climatology to obtain a smoothed annual cycle.

The variability of the stratospheric polar vortex is evaluated using the NAM index (Baldwin and Dunkerton, 2009).Variability in the strength of the stratospheric polar vortex is defined on the basis of the leading principal component (PC) time series of the daily zonal mean geopotential height anomalies at 10 hPa during the extended wintertime (November–March). We define SV and WV events by requiring the 10 hPa NAM index to be above 1 and below −1 standard deviation, respectively, for at least 15 consecutive days. The choice of 1 standard deviation represents a reasonable trade-off between event strength and sample size. The persistence criterion ensures that the NAM anomalies associated with the SV and WV events have enough time to extend toward the troposphere. Based on this approach, 29 SV events and 41 WV events are identified (as shown in Table 1). The central date of a SV or WV event (referred to as day 0) is the day with a maximal absolute value of the 10 hPa NAM index. The composite average

Table 1. Central date of SV events and WV events at 10 hPa.

Central date, strong vortex events	Central date, weak vortex events
12 January 1951	26 February 1952
10 February 1954	20 March 1954
16 February 1956	08 February 1957
15 March 1960	07 February 1958
30 December 1961	04 December 1958
10 February 1964	19 March 1959
27 February 1967	19 January 1960
27 March 1968	22 December 1960
09 February 1974	16 March 1961
11 January 1976	30 January 1963
16 January 1979	20 March 1964
26 December 1979	20 December 1965
09 January 1981	11 January 1968
10 January 1983	04 December 1968
28 January 1984	05 January 1970
12 February 1988	20 January 1971
19 January 1989	04 February 1973
28 December 1989	25 December 1976
18 January 1993	11 January 1977
12 March 1995	01 March 1980
30 December 1995	03 March 1984
19 March 1997	31 December 1984
13 January 2000	26 January 1987
18 January 2005	12 December 1987
10 December 2006	14 March 1988
10 January 2009	23 February 1989
10 January 2010	05 February 1995
16 March 2011	08 January 1998
12 December 2011	18 December 1998
	08 March 1999
	20 December 2000
	30 December 2001
	18 February 2002
	18 January 2003
	09 January 2004
	16 March 2005
	26 January 2006
	29 January 2009
	30 January 2010
	23 January 2012
	17 January 2013

of these 29 and 41 events is used to represent the life cycle of the SV and WV events, respectively. As in Limpasuvan *et al.* (2004), we present the life cycle by dividing it into five 15-day average intervals that reflect the onset (days −37 to −23), growth (days −22 to −8), maturation (days −7 to +7), decline (days +8 to +22), and decay (days +23 to +37) of a typical SV or WV event. The negative and positive signs indicate days prior to and after the central date, respectively. It should be pointed out that we also identified the SV and WV events based on the method in Limpasuvan *et al.* (2004, 2005) and found that the composited results are not sensitive to the methods for identifying SV and WV events.

The definition of the blocking index combines the traditional approaches used by Tibaldi and Molteni (1990) and the modified approaches of Scherrer *et al.* (2006) which can be applied in both latitude and longitude. The bi-dimensional index is based on the 500 hPa geopotential height gradient. The equatorward and poleward meridional gradients of geopotential height are estimated as follows, respectively.

$$\Delta_{\mathrm{eqw}} = \frac{Z500(\lambda_0,\phi_0) - Z500(\lambda_0,\phi_s)}{\phi_0 - \phi_s}, \tag{1}$$

$$\Delta_{\mathrm{plw}} = \frac{Z500(\lambda_0,\phi_n) - Z500(\lambda_0,\phi_0)}{\phi_n - \phi_0}, \tag{2}$$

where ϕ_0 ranges from 30°N to 75°N, λ_0 ranges from 0° to 360°. $\phi_s = \phi_0 - 15°$, and $\phi_n = \phi_0 + 15°$. An instantaneous blocking event is identified when the following condition is fulfilled:

$$\Delta_{\mathrm{eqw}} < 0, \quad \Delta_{\mathrm{plw}} > -10\,\mathrm{m}/°\mathrm{lat}. \tag{3}$$

The instantaneous blocking index is defined as a value of 1 on days when condition (3) is fulfilled and 0 otherwise. A comparison for different atmospheric blocking indexes can be found in Scherrer *et al.* (2006). To ensure that the blocking has sufficient spatial and temporal scales, as in Davini *et al.* (2012, 2014a), we apply the same constraints to the aforementioned instantaneous blocking index.

To analyse the effect of tropospheric blockings on the variation in upward fluxes of planetary waves, following Nishii *et al.* (2009), we treat the meridional heat flux anomalies at 100 hPa, averaged between 45°N and 75°N, as the variability of upward planetary wave fluxes. The anomalous meridional heat flux $[v^*T^*]_a$ associated with tropospheric blockings from the 5-day low-pass-filtered fields of meridional wind velocity (v) and temperature (T) is estimated by retaining fluctuations with periods longer than 5 days to fulfil the constraints of blocking persistence (Nishii *et al.*, 2011; Ayarzaguena *et al.*, 2015). In the anomalous meridional heat flux $[v^*T^*]_a$, the subscript 'a' denotes an anomaly from the climatology, the asterisks denote departures from their zonal means, and the brackets represent the zonal mean. According to Nishii *et al.* (2009, 2010), we decompose the anomalous meridional heat flux $[v^*T^*]_a$ at 100 hPa into three contribution terms:

$$[v^*T^*]_a = [v_c^*T_a^*] + [v_a^*T_c^*] + [v_a^*T_a^*]_a. \tag{4}$$

Here, the subscript 'c' stands for the daily climatological mean. The first two terms on the right-hand side of Eq. (4) represent contributions from the interference between the climatological mean planetary waves and the wave anomalies associated with blocking and are usually referred to as the linear wave interference terms. The schematic of linear interference can also be found in Fig. 1 of Smith and Kushner (2012). The term $[v_a^*T_a^*]_a$ represents the contribution from anomalous waves themselves and is usually called a nonlinear wave interference term.

A two-sided Student's *t*-test is used to assess statistical significance in this study. The number of independent samples is estimated using equation (31) in Bretherton *et al.* (1999). In the following, only the anomalies which are statistically significant at the 95% level are discussed unless otherwise stated.

3. Features of the SV (WV) events and tropospheric blockings

Figure 1 shows the composite evolution of the anomalous zonal-mean zonal wind (contours) and zonal-mean temperature (shaded) during the life cycle of SV (a–e) and WV (f–j) events. During the onset stage of SV events (Figure 1(a)), the zonal-mean zonal wind in the extratropical stratosphere is anomalously strong poleward of 50°N. Compared with the onset stage, there are intensified zonal-mean easterly wind anomalies at approximately 35°N and the zonal-mean westerly wind anomalies approximately at 60°N during the growth stage (Figure 1(b)) of SV events. In the maturation stage (Figure 1(c)), the zonal-mean zonal wind anomalies and temperature anomalies reach maxima in the polar stratosphere. The strong cold zonal-mean temperature anomalies also descend to near the tropopause. In the decline stage (Figure 1(d)), the westerly wind anomalies weaken considerably over the polar stratosphere. However, the easterly wind anomalies at approximately 35°N strengthen in the troposphere. The zonal-mean zonal wind anomalies that had reached the surface now recede upwards in the decay stage (Figure 1(e)). In addition, the diminishing centre of the cold temperature anomalies continues to descend over the polar region near 200 hPa with an anomalous temperature dipole structure. These essential features of these SV events are consistent with the results of Limpasuvan *et al.* (2005).

During the onset stage in WV events (Figure 1(f)), the zonal-mean zonal wind is anomalously strong poleward of 60°N, with

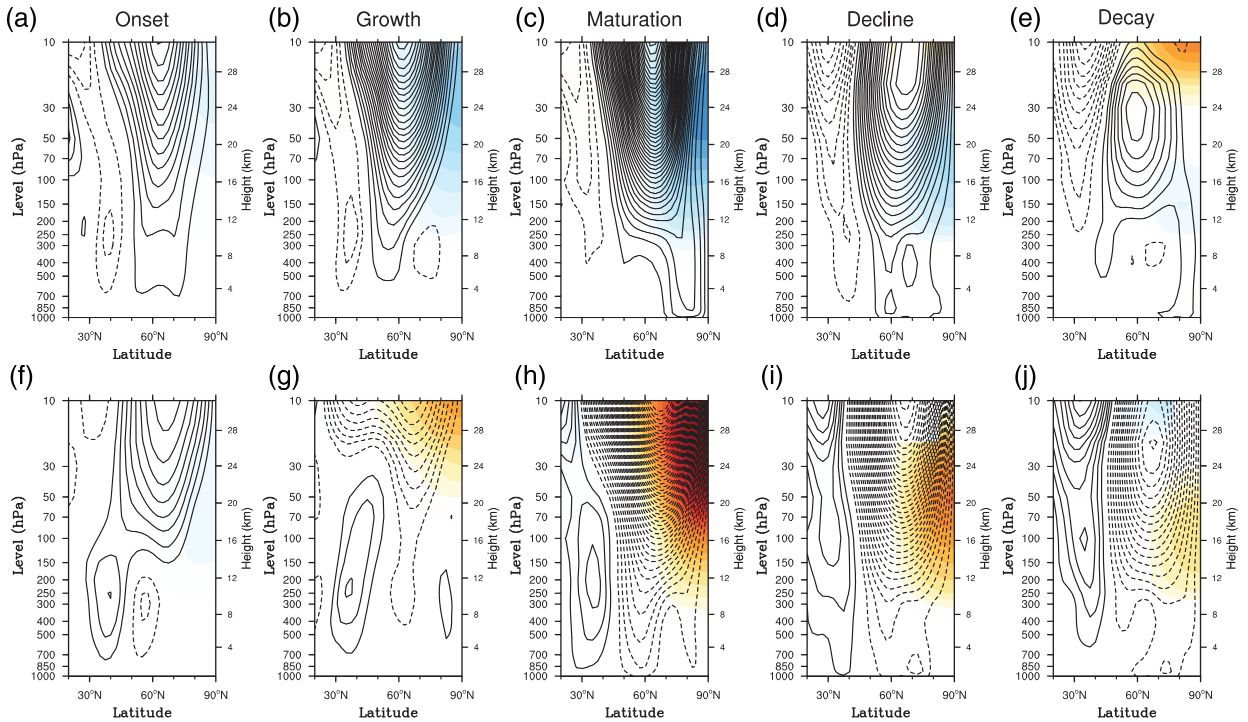

Figure 1. Latitude–pressure sections of anomalous zonal-mean zonal wind (in m s^{-1} contours; contour interval of 0.5 m s^{-1}; positive and negative contours are represented by solid and dashed lines, respectively; zero contours are omitted) and zonal-mean temperature (in K with filled contours; contour interval is 1 K) for SV (a–e) and WV (f–j) events. [Colour figure can be viewed at wileyonlinelibrary.com].

weak cold zonal-mean temperature anomalies over the polar stratosphere. This pattern is consistent with the findings of Limpasuvan *et al.* (2004). A transition from westerly wind anomalies to easterly wind anomalies is observed during the growth stage (Figure 1(g)). In the maturation and decline stages (Figures 1(h) and (i)), westerly wind anomalies at approximately 35°N and easterly wind anomalies at approximately 60°N descend gradually towards the troposphere. In the decay stage (Figure 1(j)), warm temperature anomalies descend in altitude, with maxima near 100 hPa. A temperature dipole pattern, which is opposite to that in the decay stage of SV events, can be observed over the polar region.

To show the details of anomalous blocking pattern during SV and WV events, the pattern of blocking frequency anomalies at each stage of the life cycle of SV and WV events are shown in Figure 2. The blocking frequency anomalies are calculated by subtracting the daily multiannual mean, smoothed with a 31-day running mean, from the index of blocking and then multiplying by 100%.

During the onset stage of SV events (Figure 2(a)), a decreased blocking frequency occurs predominantly over Greenland, Iceland and northern Europe, with greatest decrease over northern Europe. In addition, increased blocking frequency can be observed over parts of the northwestern Pacific, especially eastern Siberia. The pattern of blocking frequency anomalies in the growth stage (Figure 1(b)) is significantly different from that observed in the onset stage. There is a slightly increased blocking frequency over the Euro-Atlantic sector, while significantly increased blocking frequency can be found in the lower latitudes of the North Atlantic. The increased blocking frequency may not be associated with the increased blocking activity in this region (Davini *et al.*, 2012). Davini *et al.* (2012) noted a negligible impact on circulation of blocking detected south of 40°N. Thus, low-latitude blockings will not be included in the subsequent analysis. An interesting feature is that the anomalous blocking frequency pattern observed in the onset stage is significantly strengthened again when the SV events enter into the maturation stage (Figure 2(c)). Relative to the maturation stage, the blocking frequency anomalies over the eastern North Atlantic and western Europe change their signs from negative to positive during the decline stage (Figure 1(d)) and maintain the positive blocking frequency anomalies until the decay stage. There are increased blocking days around the Ural Mountains and decreased blocking days over the Bering Strait during the decline stage (Figure 1(d)).

For WV events, there are no significant changes in the frequency of the blocking events during the onset stage (Figure 2(f)). However, evident changes in blocking frequency can be found in the growth stage (Figure 2(g)) and the changes are opposite to those observed in the onset and maturation stages of SV events. Compared with SV events, an earlier change in the sign of the blocking frequency anomalies over Europe can be found during the maturation stage (Figure 1(h)) of WV events. The blocking frequency anomalies over Europe remain negative until the end of WV events. A westward shift of positive blocking frequency anomalies from northern Europe to Baffin Bay can be observed as WV events evolve and then decline. Although there are no significant changes in the blocking frequency anomalies over the western North Pacific until the end of WV events, the amplitude of negative anomalies gradually weakens.

Apart from blocking frequency changes, it is worthwhile to examine variations of the blocking intensity during the life cycle of SV and WV events. Figure 3 shows the 500 hPa geopotential height anomalies for SV and WV events. The height anomalies in Figure 3 are from the 5-day low-pass filtered fields of the 500 hPa geopotential height, which can be regarded as the blocking intensity. During the onset stage of SV events (Figure 3(a)), the negative height anomalies are found over northwestern Europe with significantly decreased blocking frequency anomalies. Positive height anomalies, which are related to the increased blocking frequency anomalies, are found over the northern North Pacific. An interesting feature is that a positive phase of NAO can be found over the North Atlantic during the decline stage. The positive NAO pattern may be related to the positive NAM anomalies extending from the stratosphere (Figure 11(a)). The increased frequency of blocking over western Europe and the decreased frequency of blocking over Iceland may be related to the positive phase of NAO. During the onset stage of WV events (Figure 3(f)), there are negative height anomalies with weak negative blocking frequency anomalies over the northern North Pacific. Positive height anomalies can be found over northwestern Eurasia. A significant negative phase of

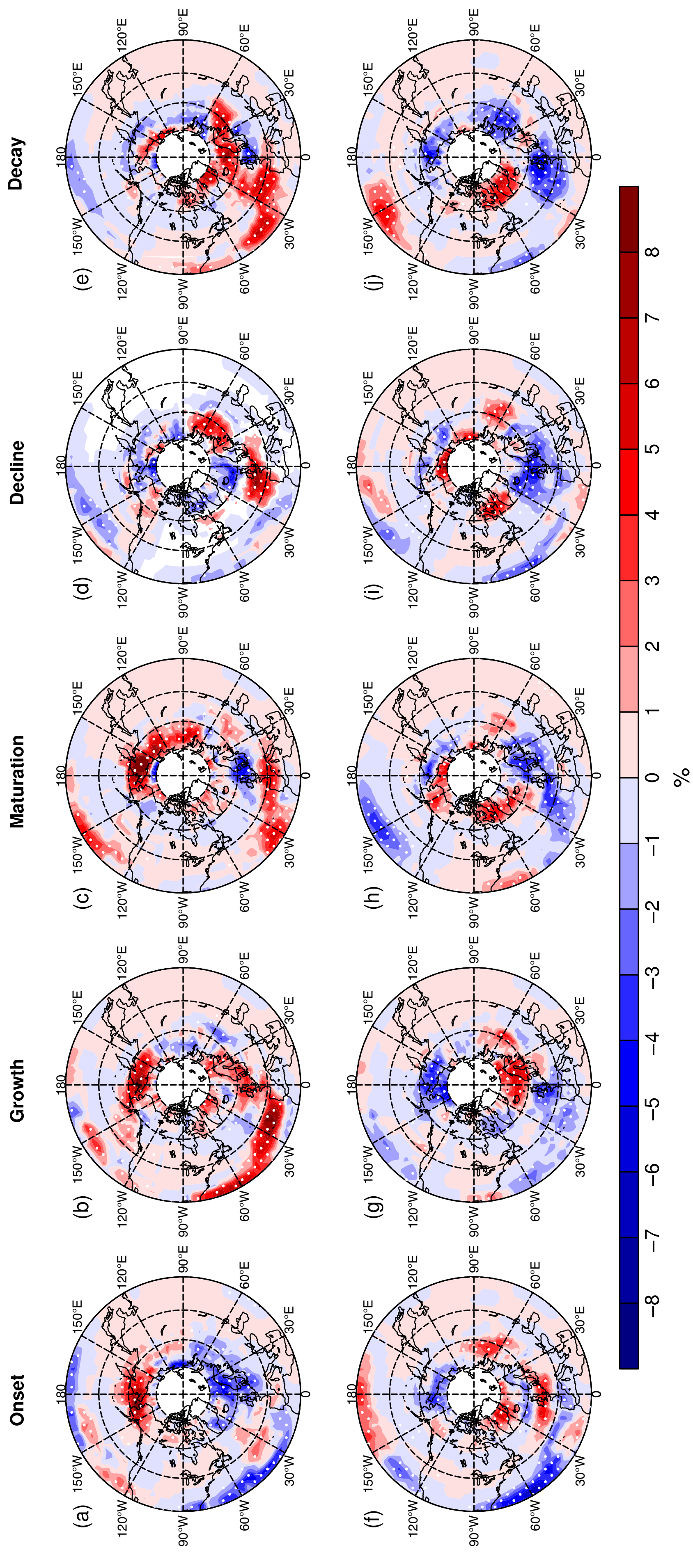

Figure 2. The composites of anomalous blocking frequency (in % with filled contours; contour interval is 1%) for SV (a–e) and WV (f–j) events. Dotting indicates areas with a 95% confidence level (based on a two-sided Student's *t*-test). [Colour figure can be viewed at wileyonlinelibrary.com].

NAO pattern, which is related to the negative NAM anomalies extending downward from the stratosphere (Figure 11(b)), can be found during the maturation and decay stages of WV events (Figures 3(h) and (j)). Previous studies also showed that the negative NAO pattern can lead to increased blocking days over Baffin Bay and decreased blocking days over the Euro-Atlantic sector (Vial *et al.*, 2013; Davini *et al.*, 2014a).

Figure 4 shows the patterns of zonal wind anomalies averaged between 925 and 700 hPa during the different stages of SV and WV events. Zonal wind speeds decrease over the upstream region of the western North Pacific during the onset and growth stages of SV events. According to Kaas and Branstator (1993), weak zonal winds are favourable for the enhanced blocking activity, thus there are increased blocking days over the western North Pacific. The positive zonal wind anomalies over the Euro-Atlantic sector are related to weakened blocking activity upstream of the Euro-Atlantic sector during the onset stage of SV events. There are positive zonal wind anomalies over the upstream region of the western North Pacific during the onset and growth stages of WV events, which tend to decrease blocking days over the western North Pacific. The increased blocking days over the Euro-Atlantic sector lead to decreases in zonal wind over the downstream region of Europe during the onset and growth stages of WV events. A significant change in the patterns of zonal wind anomalies can be found in the later stages of SV and WV events. This change may be related to the zonal wind anomalies extending from the stratosphere (Figure 1). The more detailed discussions on the impact of the changed zonal wind patterns on the distribution of blocking are presented in section 5.

4. The wave interference during the life cycle of SV and WV events

Previous studies have indicated that tropospheric blockings can affect the stratospheric polar vortex by modifying the upward fluxes of planetary waves entering the stratosphere (i.e. Quiroz, 1986; Martius *et al.*, 2009; Nishii *et al.*, 2009, 2011; Castanheira and Barriopedro, 2010). The upward fluxes of planetary waves from the troposphere to the stratosphere tend to be enhanced by the blockings over the Euro-Atlantic sector and to be weakened by the blockings over the western North Pacific. This relationship is mainly based on the phase matches between the anomalous waves forced by the tropospheric blockings and the climatological-mean planetary waves (Martius *et al.*, 2009; Nishii *et al.*, 2011). A question arises here as to whether this wave interference process is different at different stages of the life cycle of SV and WV events. To clarify this question, Figure 5 first shows the temporal–longitudinal distribution of the blocking frequency anomalies (shaded) averaged between 45°N and 75°N and also displays the climatological-mean planetary waves (wave-1 and wave-2, contours) averaged between 45°N and 75°N for SV and WV events. For SV events, from lag = −35 to −25 days, the blocking frequency is decreased over the Euro-Atlantic sector (45°W–60°E), where a climatological ridge is located. The blocking frequency is increased over the North Pacific (120–210°E), especially the northwestern North Pacific, where a climatological trough is located. There is a slight increase in the frequency of blocking over the Euro-Atlantic sector from lag = −20 to −10 days, followed by a significant decrease in the blocking frequency from lag = −10 to 0 days. In addition, a significant increase can be observed over the North Pacific from −15 to 0 days. Previous studies also pointed out that the planetary wave forcing is reduced when a blocking ridge corresponds to a climatological trough, and vice versa (Nishii *et al.*, 2011; Vial *et al.*, 2013).

The planetary wave disturbance patterns, which are decomposed by wave number using a Fourier transformation along the latitudinal circle, in the lower stratosphere are shown in Figure 6, which shows the anomalous planetary waves (contours) defined in 100 hPa geopotential height and the climatology (shaded) for SV and WV events. For SV events, the anomalies in planetary waves are almost out-of-phase with the climatological planetary waves during the onset stage (Figure 6(a)). Thus, the anomalies destructively interfere with the climatological planetary waves, leading to planetary waves with weakened amplitudes. The anomalies of planetary waves have the same signs as their climatology at most grid points during the growth stage (Figure 6(b)), which is mainly related to a slight increase in frequency of blocking over the Euro-Atlantic sector. This increase leads to a weakened destructive linear interference pattern. Although there is an in-phase superposition between the anomalies and climatology of planetary waves over Greenland, the anti-phase superposition is more evident during the maturation stage (Figure 6(c)). The results here suggest that the evolution of planetary wave disturbance patterns in the lower stratosphere is closely related to the evolution of tropospheric blockings.

Liberato *et al.* (2007) noted that negative anomalies in the meridional heat flux tend to occur when the amplitude of planetary waves is weakened. Figure 7 shows the latitude–pressure sections of the anomalous Eliassen–Palm (E-P) flux (Andrews and McIntyre, 1976) and its divergence (contours) of planetary waves (wave-1 and wave-2) for SV and WV events. During the onset and maturation stages (Figures 6(a) and (c)) of the SV events, the upward E-P fluxes are significantly reduced, and the anomalous divergences of the E-P flux occur in the high latitudes from the lower stratosphere to mid-stratosphere. As the meridional heat fluxes in the high-latitude lower stratosphere are proportional to the vertical component of E-P flux (Polvani and Waugh, 2004), the destructive interference between the climatological and anomalous waves primarily contributes to the reduced upward E-P fluxes.

For WV events (Figure 5(b)), from lag = −20 to −5 days, there are positive blocking frequency anomalies over the Euro-Atlantic sector, in which a climatological ridge is located, and negative blocking frequency anomalies over the western North Pacific, where a climatological trough is located. The anomalies of planetary waves related to tropospheric blockings in the troposphere (not shown) and stratosphere are almost in-phase with their climatology. Thus, the constructive interference between planetary wave anomalies and climatological waves strengthens the amplitude of planetary waves in the incipient stages of WV events (Figure 6(g)). As shown in Figure 7(g), the upward E-P fluxes into the stratosphere exceed their climatological values.

Based on the above analysis, tropospheric blockings can change the E-P fluxes in the stratosphere via linear wave interference. The result is consistent with the relevant results in previous studies (e.g. Orsolini *et al.*, 2009; Nishii *et al.*, 2010, 2011; Kim *et al.*, 2014). However, we can see from the above analysis that the linear interference effect in different stages of SV and WV events are not significant all the time. To examine the role of the nonlinear wave interference in the process of blockings impacting on the stratospheric polar vortex, we decompose the anomalous meridional heat flux into linear and nonlinear wave interference terms, as described in section 2. Figure 8 shows the spatial distributions of nonlinear (shaded) and linear (contours) wave interference during the different stages of SV and WV events. Note that there are statistically significant negative and positive values of the linear wave interference term at most grid points in the incipient SV (Figures 8(b) and (c)) and WV (Figures 8(g) and (h)) events, respectively. Besides, there is also a contribution from nonlinear wave interference to the anomalous upward E-P fluxes in the incipient SV and WV events. However, the positive and negative values of nonlinear wave interference term are almost comparable during the onset and growth stages of SV events.

To better understand the relative importance of linear and nonlinear wave interference during the life cycle of SV and WV events, Figure 9(a) shows the daily time series of 100 hPa eddy heat flux anomalies ($[v^{*}T^{*}]_{\mathrm{a}}$, black line) averaged over 45°N and 75°N and the contributions to the 100 hPa eddy heat flux from $[v_{\mathrm{c}}^{*}T_{\mathrm{a}}^{*}]+[v_{\mathrm{a}}^{*}T_{\mathrm{c}}^{*}]$ (red line) and $[v_{\mathrm{a}}^{*}T_{\mathrm{a}}^{*}]_{\mathrm{a}}$ (blue line) for SV

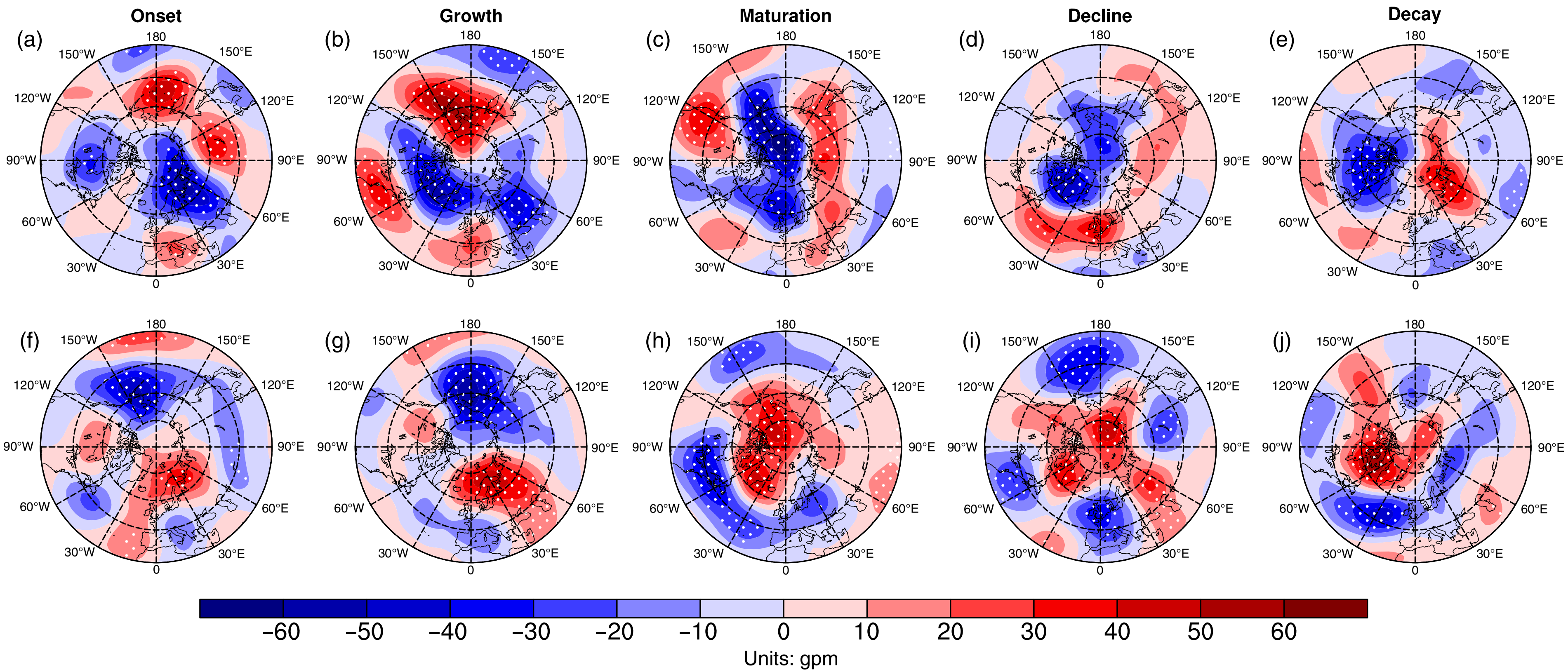

Figure 3. Composite patterns of the 500 hPa geopotential height anomaly field (in gpm with filled contours; contour interval is 20 gpm) for SV (a–e) and WV (f–j) events. Dotting indicates areas with a 95% confidence level (based on a two-sided Student's *t*-test). [Colour figure can be viewed at wileyonlinelibrary.com].

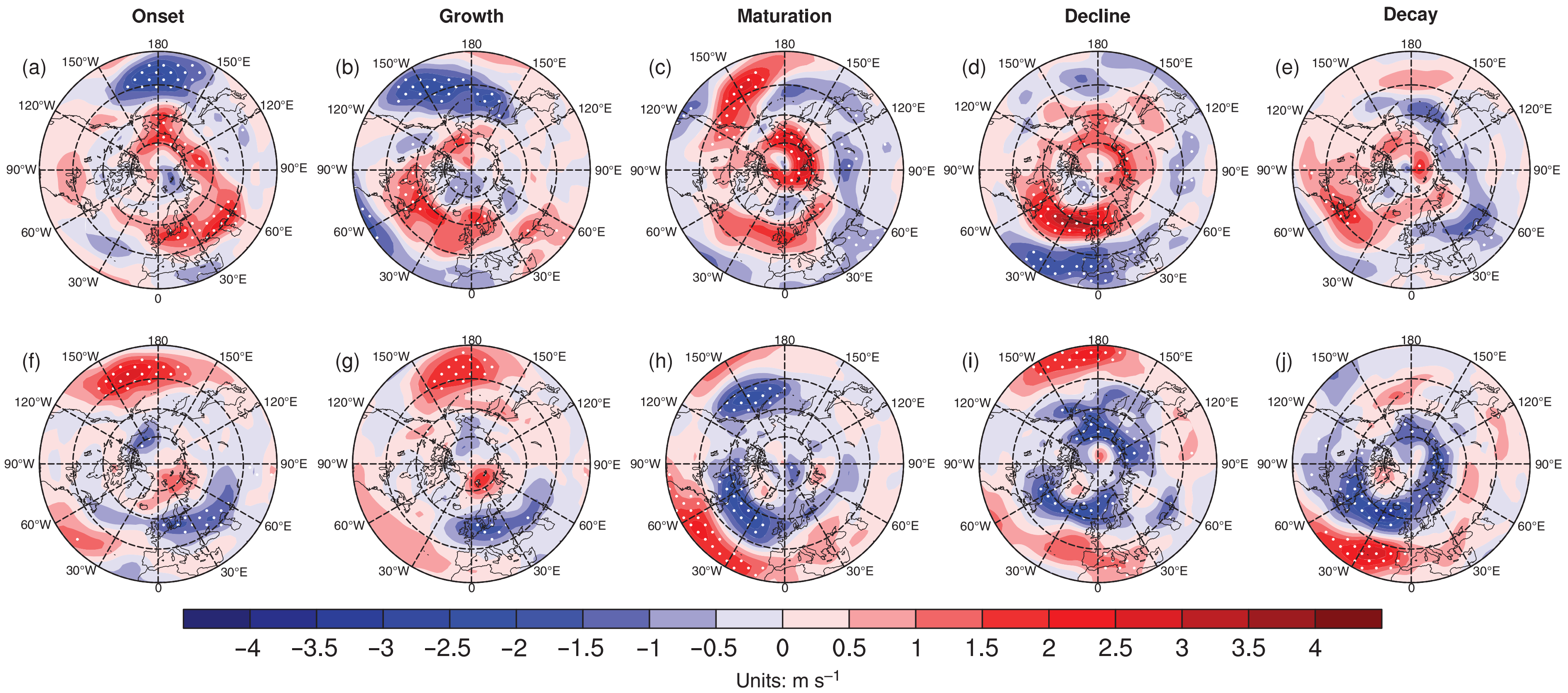

Figure 4. Composite patterns of the zonal wind anomalies averaged over 925 to 700 hPa (in m s^{-1} with filled contours; contour interval is 0.5 m s^{-1}) for SV (a–e) and WV (f–j) events. Dotting indicates areas with a 95% confidence level (based on a two-sided Student's t-test). [Colour figure can be viewed at wileyonlinelibrary.com].

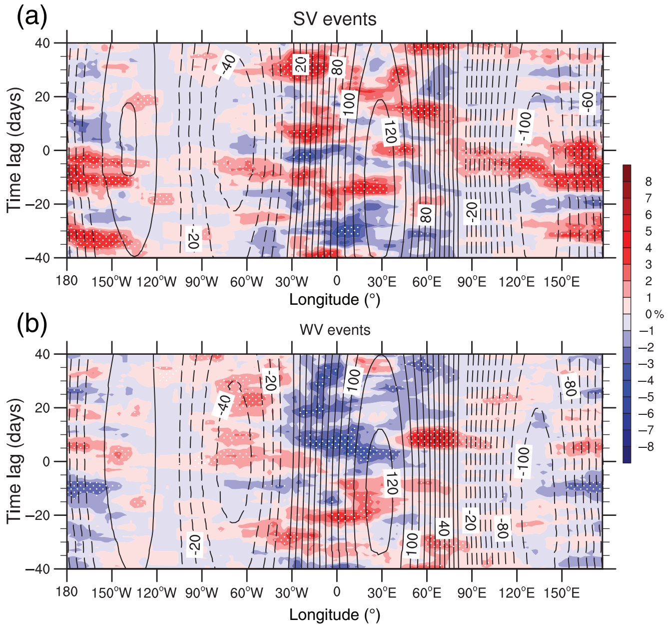

Figure 5. Temporal–longitudinal Hovmüller representation of the blocking frequency anomalies (shaded) averaged over 45–75°N for (a) SV and (b) WV events, spanning lag = −40 days to lag = +40 days (relative to the central dates; see section 2); the contour interval is 1%. Dotting indicates areas with a 95% confidence level (based on a two-sided Student's t-test). Black contours represent the composite of the climatological mean of planetary waves (planetary wave-1 and wave-2) at the 500 hPa geopotential height, averaged over 45–75°N (solid contours are positive; dashed contours are negative). [Colour figure can be viewed at wileyonlinelibrary.com].

events. The linear wave interference contributes mainly to the negative anomalies of heat flux in the onset and maturation stages of SV events, as is also evident in Figure 5(a) which indicates that the climatological ridge is overlaid by negative blocking frequency anomalies and the climatological trough is overlaid by positive blocking frequency anomalies. The nonlinear wave interference is almost equal to zero, when averaged between 45°N and 75°N, and there are no statistically significant contributions from nonlinear wave interference to heat flux anomalies in the incipient SV events. Figure 9(b) is the same as Figure 9(a) except for WV events. Figure 9(b) indicates that the linear wave interference makes a larger contribution to the positive heat flux anomalies in the growth stage of WV events than the nonlinear wave interference, as is also evident in Figure 8(g). There are no evident contributions from both the linear and nonlinear wave interference during the onset stage of WV events due to the less intense anomalous blocking pattern.

During the later stages of SV events, the amplitude of blocking frequency anomalies over the western North Pacific is weakened compared to that observed during the incipient stages of SV events. The upward fluxes of planetary waves are also significantly enhanced, accompanied by the increased blocking frequency over the Euro-Atlantic sector and the Ural Mountains, as shown in Figures 7(d) and (e). The area-averaged meridional heat fluxes present positive anomalies in the troposphere and stratosphere from lag = +5 to +30 days. There is a in-phase superposition between climatological waves and anomalous waves (Figure 6(d)); the constructive interference is mainly related to the negative blocking frequency anomalies over the western North Pacific and positive blocking frequency anomalies over the Euro-Atlantic sector and the Ural Mountains from lag = +5 to +40 days (Figure 5(a)). Figures 8(d) and (e) show that there are also statistically significant positive values in nonlinear wave interference at most grids during the decline and decays of SV events. Figure 9(a) further indicates that the nonlinear wave interference also makes a contribution to the enhanced upward fluxes of planetary waves.

For WV events, there are anomalous downward fluxes of planetary waves in the high latitudes from the troposphere to the mid-stratosphere in the decline and decay stages (Figures 7(i) and (j)) of WV events. The anomalous heat fluxes averaged between 45°N and 75°N experience significant reductions, as presented by the negative heat flux anomalies, in the troposphere and stratosphere from lag = 0 to +30 days (Figure 9(b)). The amplitude of anomalous planetary waves is weak due to less blocking days over the region north of 45°N (Figures 2(i) and (j)). But there is still weak out-of-phase superposition between climatological waves and anomalous waves (Figures 6(i) and (j)). As shown in Figures 8(i) and (j), although there are negative and positive values of linear wave interference term over the western North Pacific and Alaska, respectively, the net effect of linear interference on the heat flux anomalies is almost equal to zero when averaged over 45–75°N. There are evident contributions from the nonlinear wave interference to the negative heat flux anomalies (Figures 8(i) and (j)). Figure 9(b) indicates that the weakened upward fluxes of planetary waves are mainly related to the negative anomalies in nonlinear wave interference in the decline stage of WV events.

Considering that the SV and WV events have different time-scales, we divide SV and WV events into longer and shorter time-scale events and examine the evolution of upward heat flux in the stratosphere and the distribution of the tropospheric blockings. A WV event is regarded as a longer (shorter) time-scale event, when its duration is above (below) the 60th (40th) percentile of the duration for all WV events. A longer (shorter) SV event is identified in like manner. We find that the time evolution of the upward heat flux in the stratosphere during shorter time-scale events is overall similar to that during longer time-scale events (Figure 9). However, there are statistically significant negative heat flux anomalies in the onset stage of longer SV events but not in shorter SV events. Meanwhile, the amplitude of negative heat flux anomalies during shorter SV events is larger than that during longer SV events between lag = −10 days and lag = 0 days. After the central date, there are larger positive heat flux anomalies during shorter SV events than during longer SV events. Compared to shorter WV events, the positive heat flux anomalies before the central date are larger and negative heat flux anomalies are more persistent during longer WV events (Figures 9(d) and (f)).

Figure 10 shows the distribution of blocking frequency anomalies during shorter and longer SV and WV events averaged over growth and pre-maturation stage (lag = −22 to −1 days) and averaged over post-maturation and decline stage (lag = 1–22 days). Note that before the central date, the amplitude of blocking frequency anomalies over the western North Pacific during shorter SV events (Figure 10(a)) are overall larger than those during longer SV events (Figure 10(b)). On the other hand, there are fewer blocking days over western Europe during shorter SV events than those during longer SV events. After the central date, there are more blocking days during shorter SV events over the Ural Mountains and fewer blocking days over Baffin Bay (Figure 10(c)). During longer SV events (Figure 10(d)), there are more blocking days over western Europe and fewer blocking days over Baffin Bay. However, there are no differences in the patterns of blocking frequency anomalies over the North Pacific between shorter and longer SV events.

Before the central date, the amplitude of negative blocking frequency anomalies over the western North Pacific during shorter WV events (Figure 10(e)) is larger than that during longer WV events (Figure 10(f)). Accordingly, there are positive blocking frequency anomalies over the Ural Mountains during shorter WV events, while there are positive blocking frequency anomalies over the northeastern North Atlantic and northern Europe during longer WV events. After the central date, there are negative blocking frequency anomalies over the Euro-Atlantic sector during both shorter and longer WV events, but there are more blocking days over Greenland during longer WV events. There are no differences in the blocking frequency over the North Pacific between shorter and longer WV events.

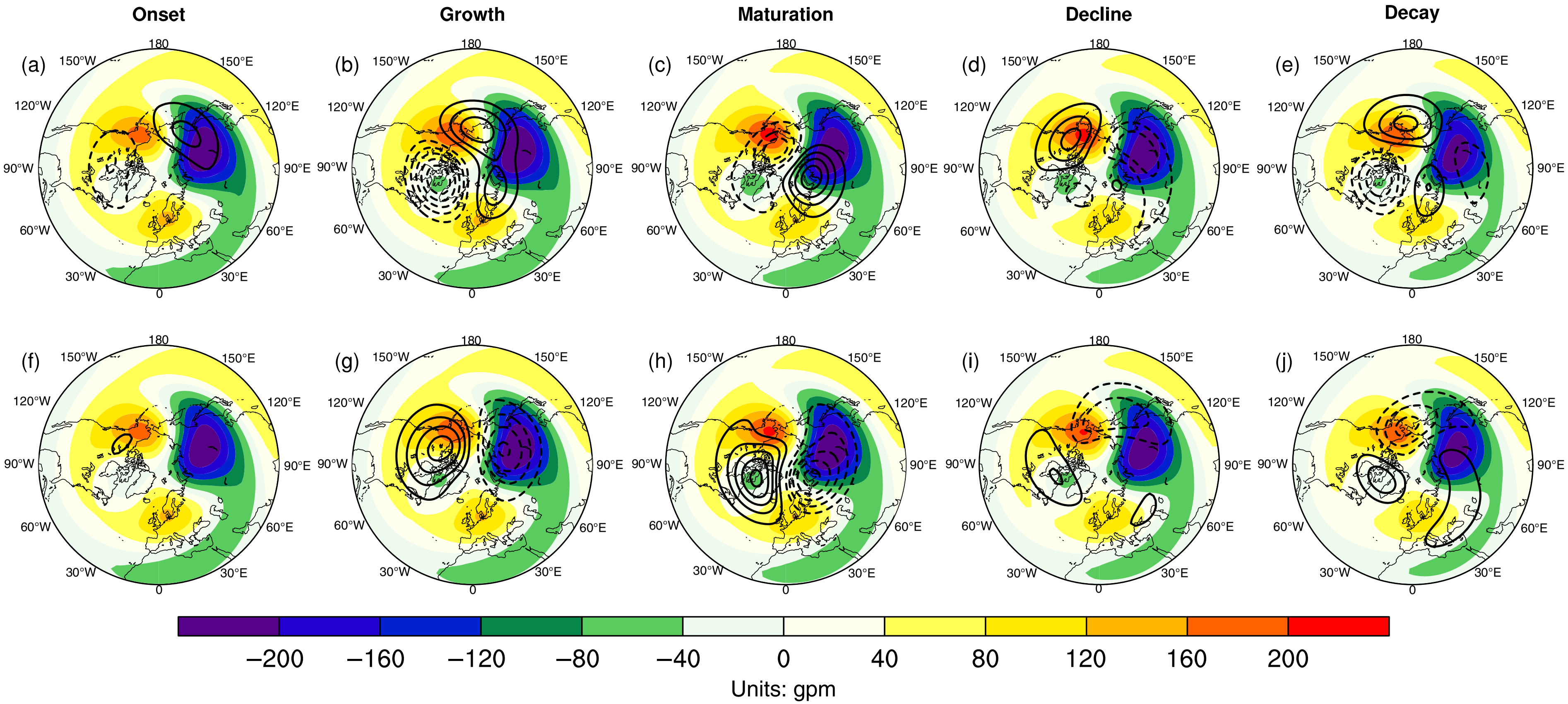

Figure 6. The climatological planetary waves (planetary wave-1 and wave-2; shading; the contour interval is 40 gpm) and the planetary wave anomalies from the climatology (contours; the contour interval is 20 gpm, and zero contours are omitted, with positive in solid and negative in dashed) in geopotential height fields at 100 hPa for SV (a–e) and WV (f–j) events. [Colour figure can be viewed at wileyonlinelibrary.com].

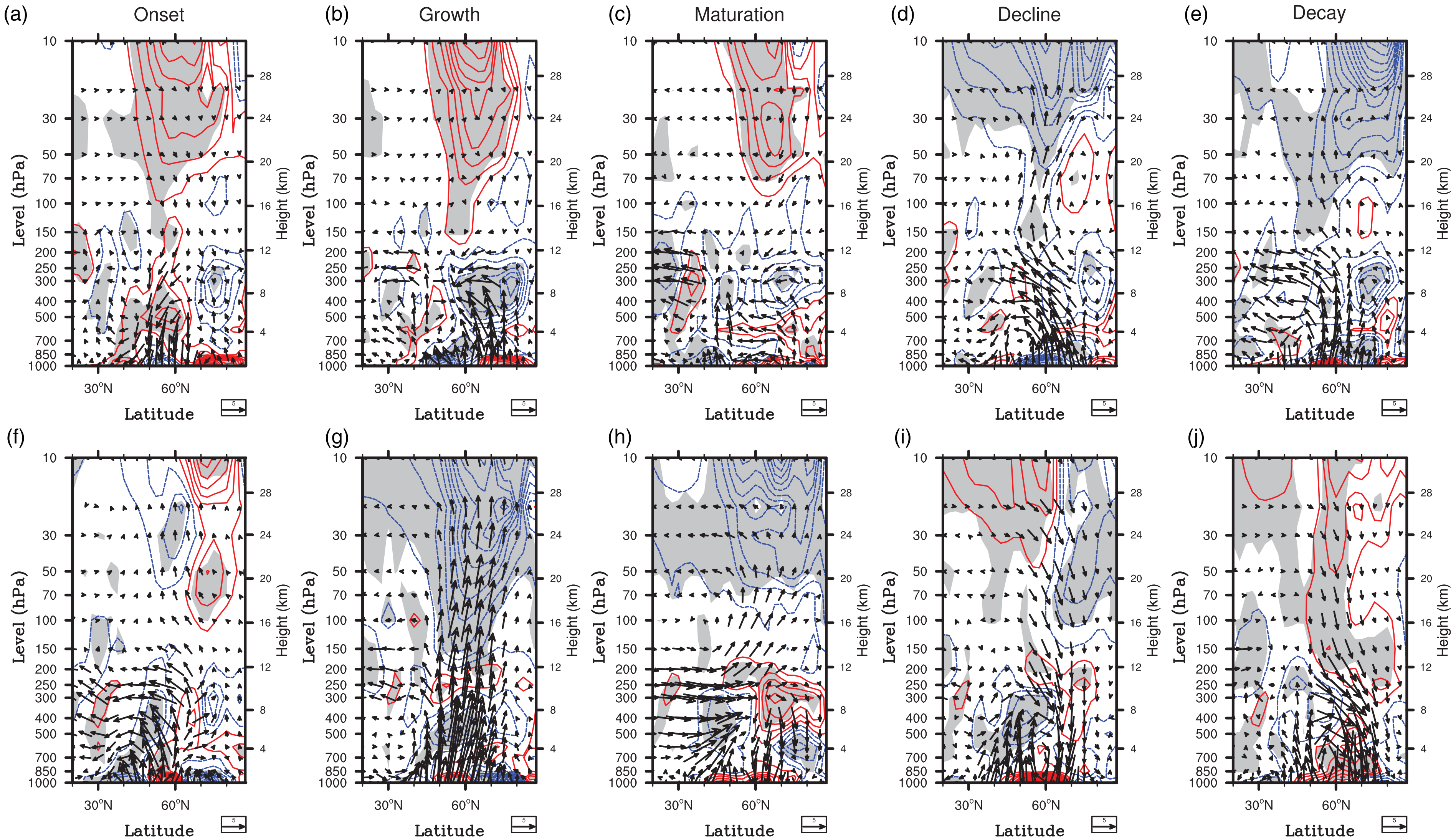

Figure 7. Latitude–pressure sections of anomalous E-P flux (arrows) and its divergence (contours) of planetary waves (planetary wave-1 and wave-2) for the (a–e) SV and (f–j) WV events. The meridional component (F_y) and the vertical component (F_z) of the E-P flux are divided by 10^{-6} and 10^{-4} before the composites, respectively. The vector lengths of the E-P flux are shown in the bottom-right of each plot, 5 kg s^{-2}. The contour interval is 0.3 m s^{-1} day^{-1} for the divergence of the E-P flux. Negative and positive contours are given as blue dashed lines and red solid lines, respectively. Zero contours are omitted. Grey shading indicates areas with a 95% confidence level (based on a two-sided Student's t-test). [Colour figure can be viewed at wileyonlinelibrary.com].

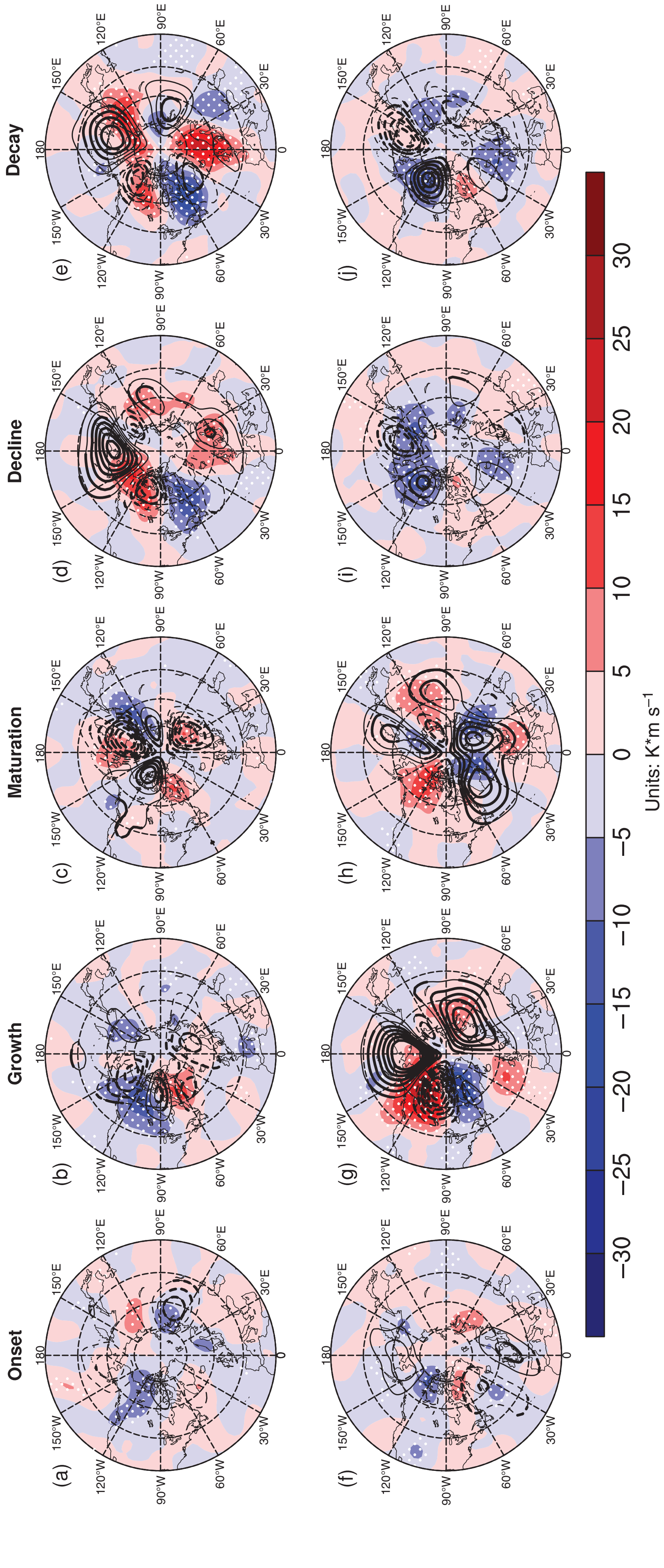

Figure 8. The spatial patterns of linear (contours) and nonlinear (shaded) wave interference for (a–e) SV and (f–j) WV events. The contour interval is 5 K m s^{-1}. Zero contours are omitted. Bold contours and dotting indicates areas with a 95% confidence level (based on a two-sided Student's *t*-test). [Colour figure can be viewed at wileyonlinelibrary.com].

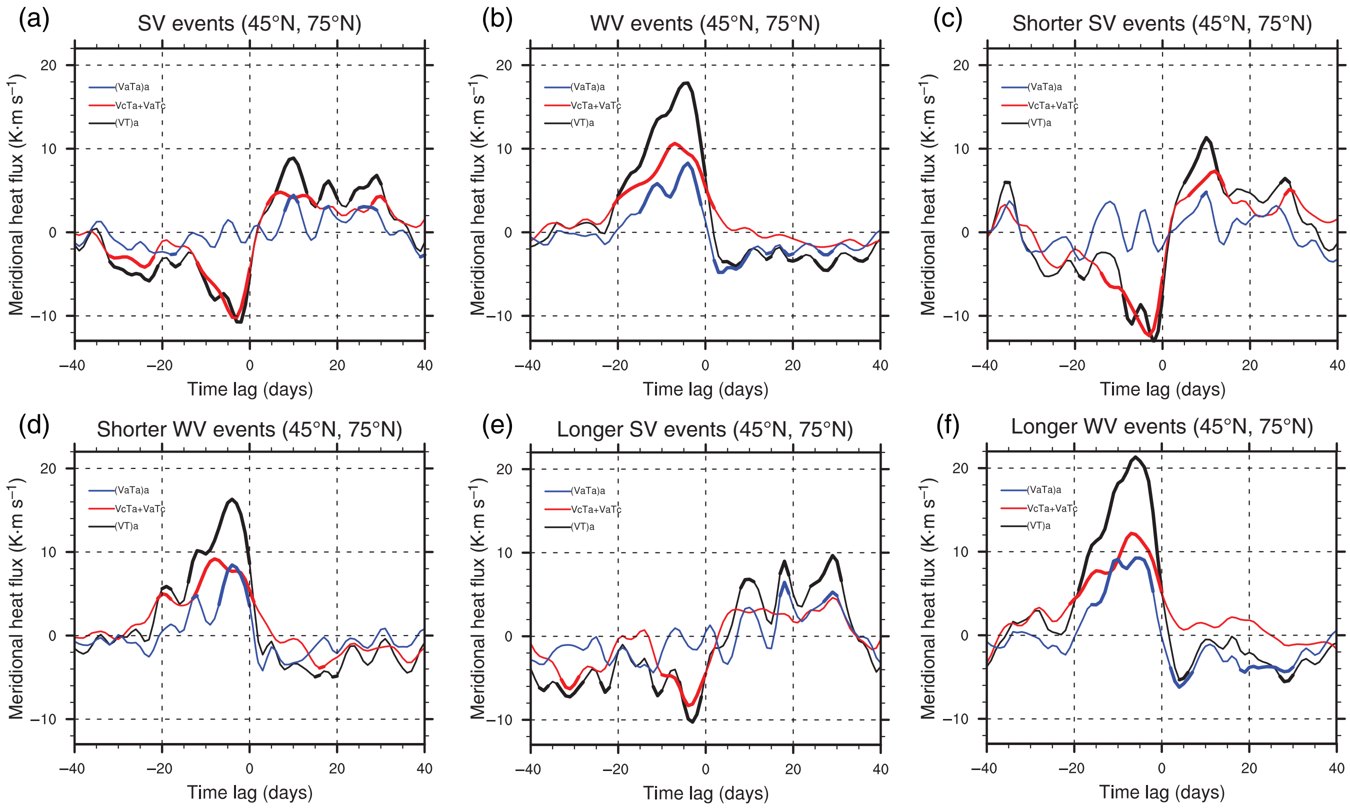

Figure 9. (a) Composited daily time series of 100 hPa anomalous meridional heat flux, which is calculated from the 5-day low-pass filtered fields of meridional velocity (v) and temperature (T) ($[v^*T^*]_a$, black line), averaged between 45°N and 75°N, and the contributions to the 100 hPa anomalous heat flux from $[v_c^*T_a^* + v_a^*T_c^*]$ (red line) and $[v_a^*T_a^*]_a$ (blue line) for SV events, averaged between 45°N and 75°N. (b) As in (a) but for WV events. (c) and (e) as in (a) but for shorter and longer SV events, respectively. (d) and (f) as in (b) but for shorter and longer WV events, respectively. Day zero refers to the central date of SV or WV events. Thick line segments indicate anomalies significantly different from zero at the 95% confidence level (based on a two-sided Student's t-test). [Colour figure can be viewed at wileyonlinelibrary.com].

5. The potential influences of extreme vortex events on tropospheric blockings

We can see from the analysis in section 3 that both blocking frequency and intensity change during different stage of SV and WV events while previous studies have found that SV and WV events may have an influence on the tropospheric blockings (Woollings *et al.*, 2010; Vial *et al.*, 2013; Davini *et al.*, 2014a). However, the detailed linkage between the evolution of extreme vortex events and blocking changes has not been well established so far. Here we examine the effect of zonal wind anomalies extending from the stratosphere on the tropospheric blockings. The zonal wind speed intensifies over Iceland especially during the decline stage of SV events (Figure 4(d)). At the same time, the frequency of blocking days decreases over Iceland (Figure 2(d)). The zonal wind between 30°N and 45°N over the Euro-Atlantic sector decreases, and correspondingly, there are increased blocking days over southern Europe. There is a decrease in zonal wind speed over southern Greenland after the central date of WV events (Figures 4(i) and (j)). Consequently, the blocking frequency is increased over Greenland (Figures 2(i) and (j)). In addition, the decreased blocking frequency anomalies over the Euro-Atlantic sector may be related to the positive zonal wind anomalies over upstream of the North Atlantic. There are no statistically significant blocking frequency anomalies, although negative zonal wind anomalies can be found over the eastern North Pacific during the maturation and decline stages of WV events (Figures 4(h) and (i)).

Figure 11 further shows the time–height variations in the standardized NAM index for SV and WV events. Baldwin and Dunkerton (2001) found that the NAM anomalies extending downward from the stratosphere can lead to a displacement in the tropospheric storm track, while Davini *et al.* (2014b) showed that there are increased and decreased blocking frequencies over the Euro-Atlantic sector when the eddy-driven jet stream is displaced poleward and equatorward, respectively. A poleward and equatorward displaced jet stream can lead to an increase and a decrease in anticyclonic Rossby wave breaking (Strong and Magnusdottir, 2008), respectively. The anticyclonic Rossby wave breaking can push subtropical air with low potential vorticity moving northeastward, which is favourable for the maintenance of the blocking over the Euro-Atlantic sector.

The displacements of the eddy-driven jet stream over the Atlantic sector (60°W–0°) and the Pacific sector (150–210°E) during the evolution of SV and WV events are shown in Figure 12. According to Davini *et al.* (2014b), the position of the eddy-driven jet in each sector is defined as the latitude where the zonally mean zonal winds averaged between 925 and 700 hPa reach a maximum over the Atlantic sector and the Pacific sector. We can see from Figure 12(a) that there is a poleward displacement of the eddy-driven jet stream over the Atlantic from lag = +10 to lag = +20 days accompanied by positive NAM anomalies extending from the stratosphere into the troposphere from lag = 0 days (Figure 11(a)). The results here suggest that the effect of stratospheric anomalies on the eddy-driven jet lasts for 10 days. Consequently, the blocking frequency is increased over the Euro-Atlantic sector after the central date of SV events (Figure 5(a)). There is no statistically significant displacement of the eddy-driven jet stream over the Pacific when the positive NAM anomalies extend downward from the stratosphere into the troposphere for SV events.

An equatorward displacement of the eddy-driven jet stream over the Atlantic can be found at approximately lag = 0 days for WV events (Figure 12(b), black line), which is preceded by the stratospheric negative NAM anomalies (Figure 11(b)) about 10 days. In addition, another statistically significant equatorward displacement of the eddy-driven jet stream over the Atlantic can also be found from lag = +25 to +35 days, which is related to the descending negative NAM anomalies before lag = +20 days. As depicted in Figure 4(b), there is decreased blocking frequency

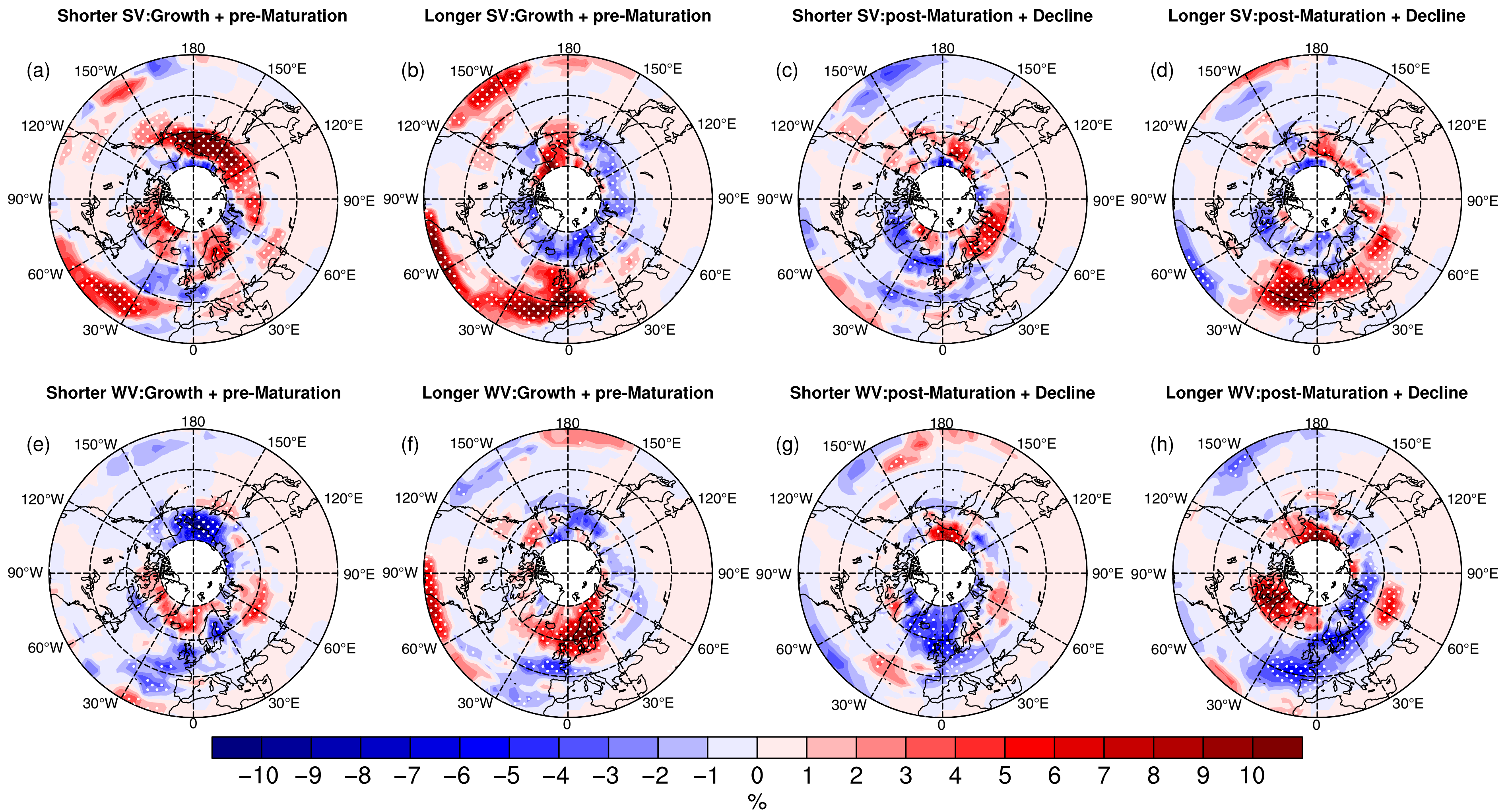

Figure 10. The composites of anomalous blocking frequency (in % with filled contours; contour interval is 1%) for shorter and longer time-scale SV (a–d) and WV (e–h) events. Dotting indicates areas with a 95% confidence level (based on a two-sided Student's *t*-test). [Colour figure can be viewed at wileyonlinelibrary.com].

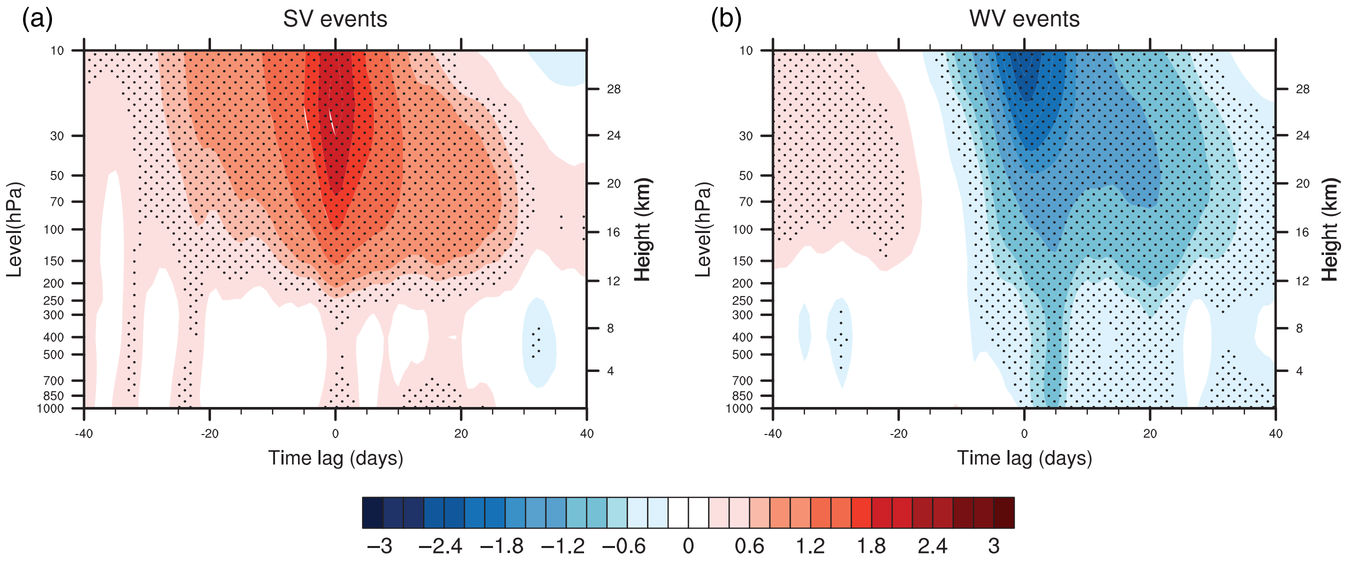

Figure 11. Composited time–height variations of the standardized NAM index for (a) SV events and (b) WV events. Dotting indicates areas with a 95% confidence level (based on a two-sided Student's t-test). [Colour figure can be viewed at wileyonlinelibrary.com].

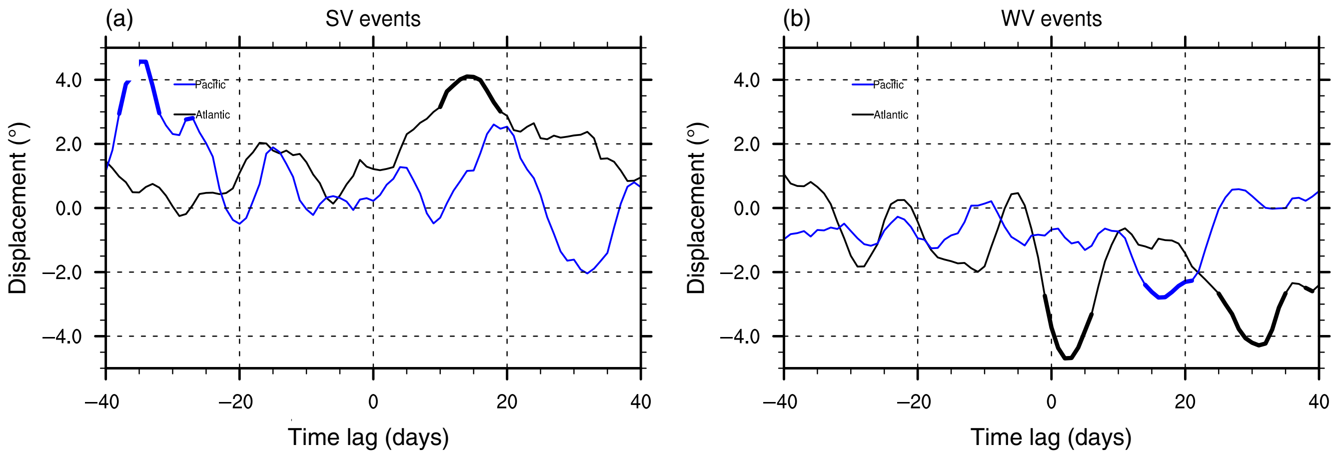

Figure 12. (a) Composited daily time series of the anomalous position of the eddy-driven jet stream over the Euro-Atlantic sector (black line, 60°W–0°) and the Pacific sector (blue line, 150–210°E) for SV events. (b) As in (a) but for WV events. Thick line segments indicate anomalies significantly different from zero at the 95% confidence level (based on a two-sided Student's t-test). See text for the details of the position of the eddy-driven jet stream. [Colour figure can be viewed at wileyonlinelibrary.com].

during the decline and decay stages of WV events and this decrease should be due to decreased anticyclonic Rossby wave breaking. A weak equatorward displacement of the eddy-driven jet stream over the Pacific can also be found around lag = +20 days and does not occur at the same time as that over the Atlantic. Note that various factors, such as the climatological position of the jet stream (Garfinkel *et al.*, 2013), eddy phase speed (Chen and Held, 2007) and planetary waves (Perlwitz and Harnik, 2003) may affect the timing of the displacements of the jet stream. Although there is an equatorward displacement of the eddy-driven jet stream over the North Pacific, the negative blocking frequency anomalies are not statistically significant. It is apparent from the above analysis that connections among stratospheric polar vortex, tropospheric blockings and eddy-driven jet stream over the North Pacific are more complex than those over the North Atlantic. Previous studies also pointed out that the response of the jet stream to stratospheric NAM anomalies is not easy to establish over the North Pacific (e.g. Garfinkel *et al.*, 2013).

6. Conclusions

The connection between extreme stratospheric polar vortex events and tropospheric blockings is analysed using a composite approach. The variations of tropospheric blockings are shown in detail at each stage of the life cycle of SV and WV events. The anomalous blocking pattern has decreased blocking days over the Euro-Atlantic sector and increased blocking days over the northern North Pacific during the onset and maturation stages of SV events. There are more blocking days over the western North Pacific during shorter time-scale SV events than during longer time-scale SV events at their maturation stage. The blocking frequency increases over the Ural Mountains and western Europe during the decline stage of SV events. The changes of the blocking frequency during the growth stage of WV events are opposite to those observed during the onset and maturation stages of SV events. There are fewer blocking days over the western North Pacific during shorter time-scale WV events, whereas there are blocking days over northern Europe during longer time-scale WV events. The blocking frequency decreases over the Euro-Atlantic sector and increases over Baffin Bay after the central date of WV events. There are no persistent changes in the anomalous blocking pattern over the North Pacific for both SV and WV events.

Our analysis reveals that the anomalous planetary waves related to tropospheric blocking constructively interfere with the climatological waves and lead to negative planetary wave flux anomalies in the stratosphere during the onset and maturation stages of SV events. This result has also been reported in the previous literature. However, our analysis further reveals that both the linear wave interference and the nonlinear interference between anomalous waves forced by the tropospheric blockings contribute to the enhanced upward fluxes of planetary waves before the central date of WV events with greater contribution from linear wave interference, and that only the nonlinear wave interference contributes to the negative planetary wave flux anomalies after the central date of WV events. During the decline and decay stage of SV events, the enhanced upward planetary wave fluxes mainly result from enhanced linear wave interference during shorter time-scale SV events and from enhanced nonlinear wave interference during longer time-scale SV events.

The NAM anomalies extending from the stratosphere can lead to a change in the tropospheric blocking frequency by modulating the position of the eddy-driven jet stream. A statistically significant poleward displaced jet stream over the Atlantic lasts for 10 days during the decline stage of SV events which is related to the descending positive NAM anomalies from lag $= -10$ days. For WV events, the descending negative NAM anomalies from lag $= -10$ to $+20$ days may cause an equatorward displacement of the eddy-driven jet stream at approximately lag $= 0$ and 25 days and then the decreased blocking frequency can be found over the Euro-Atlantic sector during the same period. In addition, the changes in the patterns of blocking frequency anomalies are closely related to the descending stratospheric zonal wind anomalies.

Acknowledgements

This work is supported by the National Science Foundation of China (41630421, 41575038, 41521004, 41405041). We greatly appreciate three anonymous reviewers and editors for their constructive comments and suggestions. We thank the scientific teams at NCEP and NCAR for providing the reanalysis data. Finally, we also appreciate the College of Atmospheric Sciences, Lanzhou University for providing the computing support.

References

Andrews DG, McIntyre ME. 1976. Planetary waves in horizontal and vertical shear: the generalized Eliassen–Palm relation and the mean zonal acceleration. *J. Atmos. Sci.* **33**: 2031–2048, doi: 10.1175/1520-0469(1976)033<2031:PWIHAV>2.0.CO;2.

Andrews DG, Holton JR, Leovy CB. 1987. *Middle Atmosphere Dynamics*. Academic Press/Elsevier: Cambridge, MA.

Ayarzaguena B, Orsolini YJ, Langematz U, Abalichin J, Kubin A. 2015. The relevance of the location of blocking highs for stratospheric variability in a changing climate. *J. Clim.* **28**: 531–549, doi: 10.1175/JCLI-D-14-00210.1.

Baldwin MP, Dunkerton TJ. 1999. Propagation of the Arctic Oscillation from the stratosphere to the troposphere. *J. Geophys. Res.* **104**: 30937–30946, doi: 10.1029/1999JD900445.

Baldwin MP, Dunkerton TJ. 2001. Stratospheric harbingers of anomalous weather regimes. *Science* **294**: 581–584, doi: 10.1126/science.1063315.

Baldwin MP, Thompson DWJ. 2009. A critical comparison of stratosphere–troposphere coupling indices. *Q. J. R. Meteorol. Soc.* **135**: 1661–1672, doi: 10.1002/qj.479.

Barriopedro D, Garcia-Herrera R, Lupo AR, Hernandez E. 2006. A climatology of Northern Hemisphere blocking. *J. Clim.* **19**: 1042–1063, doi: 10.1175/JCLI3678.1.

Black RX. 2002. Stratospheric forcing of surface climate in the Arctic Oscillation. *J. Clim.* **15**: 268–277, doi: 10.1175/1520-0442(2002)015<0268:Sfosci>2.0.Co;2.

Black RX, McDaniel BA. 2004. Diagnostic case studies of the northern annular mode. *J. Clim.* **17**: 3990–4004, doi: 10.1175/1520-0442(2004)017<3990:Dcsotn>2.0.Co;2.

Bretherton CS, Widmann M, Dymnikov VP, Wallace JM, Blade I. 1999. The effective number of spatial degrees of freedom of a time-varying field. *J. Clim.* **12**: 1990–2009, doi: 10.1175/1520-0442(1999)012<1990:TENOSD>2.0.CO;2.

Castanheira JM, Barriopedro D. 2010. Dynamical connection between tropospheric blockings and stratospheric polar vortex. *Geophys. Res. Lett.* **37**: L13809, doi: 10.1029/2010GL043819.

Charlton AJ, Polvani LM. 2007. A new look at stratospheric sudden warmings. Part I: Climatology and modeling benchmarks. *J. Clim.* **20**: 449–469, doi: 10.1175/JCLI3996.1.

Charney JG, Drazin PG. 1961. Propagation of planetary-scale disturbances from the lower to the upper atmosphere. *J. Geophys. Res.* **66**: 83–109, doi: 10.1029/JZ066i001p00083.

Chen G, Held IM. 2007. Phase speed spectra and the recent poleward shift of Southern Hemisphere surface westerlies. *Geophys. Res. Lett.* **34**: L21805, doi: 10.1029/2007GL031200.

Chen W, Yang S, Huang RH. 2005. Relationship between stationary planetary wave activity and the East Asian winter monsoon. *J. Geophys. Res.* **110**: D14110, doi: 10.1029/2004JD005669.

Croci-Maspoli M, Schwierz C, Davies HC. 2007. A multifaceted climatology of atmospheric blocking and its recent linear trend. *J. Clim.* **20**: 633–649, doi: 10.1175/JCLI4029.1.

Davini P, Cagnazzo C, Gualdi S, Navarra A. 2012. Bidimensional diagnostics, variability, and trends of Northern Hemisphere blocking. *J. Clim.* **25**: 6496–6509, doi: 10.1175/JCLI-D-12-00032.1.

Davini P, Cagnazzo C, Anstey JA. 2014a. A blocking view of the stratosphere–troposphere coupling. *J. Geophys. Res.* **119**: 11100–11115, doi: 10.1002/2014JD021703.

Davini P, Cagnazzo C, Fogli PG, Manzini E, Gualdi S, Navarra A. 2014b. European blocking and Atlantic jet stream variability in the NCEP/NCAR reanalysis and the CMCC-CMS climate model. *Clim. Dyn.* **43**: 71–85, doi: 10.1007/s00382-013-1873-y.

Garfinkel CI, Waugh DW, Gerber EP. 2013. The effect of tropospheric jet latitude on coupling between the stratospheric polar vortex and the troposphere. *J. Clim.* **26**: 2077–2095, doi: 10.1175/JCLI-D-12-00301.1.

Hartley DE, Villarin JT, Black RX, Davis CA. 1998. A new perspective on the dynamical link between the stratosphere and troposphere. *Nature* **391**: 471–474, doi: 10.1038/35112.

Hitchcock P, Simpson IR. 2014. The downward influence of stratospheric sudden warmings. *J. Atmos. Sci.* **71**: 3856–3876, doi: 10.1175/JAS-D-14-0012.1.

Kaas E, Branstator G. 1993. The relationship between a zonal index and blocking activity. *J. Atmos. Sci.* **50**: 3061–3077, doi: 10.1175/1520-0469(1993)050,3061:TRBAZI.2.0.CO;2.

Kim BM, Son SW, Min SK, Jeong JH, Kim SJ, Zhang XD, Shim T, Yoon JH. 2014. Weakening of the stratospheric polar vortex by Arctic sea-ice loss. *Nat. Commun.* **5**: 4646, doi: 10.1038/ncomms5646.

Kodera K, Mukougawa H, Fujii A. 2013. Influence of the vertical and zonal propagation of stratospheric planetary waves on tropospheric blockings. *J. Geophys. Res.* **118**: 8333–8345, doi: 10.1002/jgrd.50650.

Kolstad EW, Breiteig T, Scaife AA. 2010. The association between stratospheric weak polar vortex events and cold air outbreaks in the Northern Hemisphere. *Q. J. R. Meteorol. Soc.* **136**: 886–893, doi: 10.1002/qj.620.

Kuroda Y. 2008. Effect of stratospheric sudden warming and vortex intensification on the tropospheric climate. *J. Geophys. Res.* **113**: D15110, doi: 10.1029/2007JD009550.

Liberato MLR, Castanheira JM, de la Torre L, DaCamara CC, Gimeno L. 2007. Wave energy associated with the variability of the stratospheric polar vortex. *J. Atmos. Sci.* **64**: 2683–2694, doi: 10.1175/jas3978.1.

Limpasuvan V, Thompson DWJ, Hartmann DL. 2004. The life cycle of the Northern Hemisphere sudden stratospheric warmings. *J. Clim.* **17**: 2584–2596, doi: 10.1175/1520-0442(2004)017<2584:Tlcotn>2.0.Co;2.

Limpasuvan V, Hartmann DL, Thompson DWJ, Jeev K, Yung YL. 2005. Stratosphere–troposphere evolution during polar vortex intensification. *J. Geophys. Res.* **110**: D24101, doi: 10.1029/2005JD006302.

Lu CH, Ding YH. 2013. Observational responses of stratospheric sudden warming to blocking highs and its feedbacks on the troposphere. *Chin. Sci. Bull.* **58**: 1374–1384, doi: 10.1007/s11434-012-5505-4.

McIntyre ME. 1982. How well do we understand the dynamics of stratospheric warmings. *J. Meteorol. Soc. Jpn.* **60**: 37–65.

Marshall AG, Scaife AA. 2010. Improved predictability of stratospheric sudden warming events in an atmospheric general circulation model with enhanced stratospheric resolution. *J. Geophys. Res.* **115**: D16114, doi: 10.1029/2009JD012643.

Martius O, Polvani LM, Davies HC. 2009. Blocking precursors to stratospheric sudden warming events. *Geophys. Res. Lett.* **36**: L14806, doi: 10.1029/2009GL038776.

Matsuno T. 1971. A dynamical model of the stratospheric sudden warming. *J. Atmos. Sci.* **28**: 1479–1494, doi: 10.1175/1520-0469(1971)028<1479:ADMOTS>2.0.CO;2.

Mitchell DM, Gray LJ, Anstey J, Baldwin MP, Charlton-Perez AJ. 2013. The influence of stratospheric vortex displacements and splits on surface climate. *J. Clim.* **26**: 2668–2682, doi: 10.1175/jcli-D-12-00030.1.

Mukougawa H, Hirooka T. 2004. Predictability of stratospheric sudden warming: A case study for 1998/99 winter. *Mon. Weather Rev.* **132**: 1764–1776, doi: 10.1175/1520-0493(2004)132<1764:Posswa>2.0.Co;2.

Mukougawa H, Sakai H, Hirooka T. 2005. High sensitivity to the initial condition for the prediction of stratospheric sudden warming. *Geophys. Res. Lett.* **32**: L17806, doi: 10.1029/2005GL022909.

Nakagawa KI, Yamazaki K. 2006. What kind of stratospheric sudden warming propagates to the troposphere? *Geophys. Res. Lett.* **33**: L04801, doi: 10.1029/2005GL024784.

Nishii K, Nakamura H, Miyasaka T. 2009. Modulations in the planetary wave field induced by upward-propagating Rossby wave packets prior to stratospheric sudden warming events: a case-study. *Q. J. R. Meteorol. Soc.* **135**: 39–52, doi: 10.1002/qj.359.

Nishii K, Nakamura H, Orsolini YJ. 2010. Cooling of the wintertime Arctic stratosphere induced by the western Pacific teleconnection pattern. *Geophys. Res. Lett.* **37**: L13805, doi: 10.1029/2010GL043551.

Nishii K, Nakamura H, Orsolini YJ. 2011. Geographical dependence observed in blocking high influence on the stratospheric variability through enhancement and suppression of upward planetary-wave propagation. *J. Clim.* **24**: 6408–6423, doi: 10.1175/jcli-D-10-05021.1.

Orsolini YJ, Karpechko AY, Nikulin G. 2009. Variability of the Northern Hemisphere polar stratospheric cloud potential: the role of North Pacific disturbances. *Q. J. R. Meteorol. Soc.* **135**: 1020–1029, doi: 10.1002/qj.409.

Perlwitz J, Graf HF. 2001. Troposphere–stratosphere dynamic coupling under strong and weak polar vortex conditions. *Geophys. Res. Lett.* **28**: 271–274, doi: 10.1029/2000GL012405.

Perlwitz J, Harnik N. 2003. Observational evidence of a stratospheric influence on the troposphere by planetary wave reflection. *J. Clim.* **16**: 3011–3026, doi: 10.1175/1520-0442(2003)016<3011:OEOASI>2.0.CO;2.

Polvani LM, Kushner PJ. 2002. Tropospheric response to stratospheric perturbations in a relatively simple general circulation model. *Geophys. Res. Lett.* **29**: 1114, doi: 10.1029/2001GL014284.

Polvani LM, Waugh DW. 2004. Upward wave activity flux as a precursor to extreme stratospheric events and subsequent anomalous surface weather regimes. *J. Clim.* **17**: 3548–3554, doi: 10.1175/1520-0442(2004)017<3548: Uwafaa>2.0.Co;2.

Quiroz RS. 1986. The association of stratospheric warmings with tropospheric blocking. *J. Geophys. Res.* **91**: 5277–5285, doi: 10.1029/JD091id04p05277.

Scherrer SC, Croci-Maspoli M, Schwierz C, Appenzeller C. 2006. Two-dimensional indices of atmospheric blocking and their statistical relationship with winter climate patterns in the Euro-Atlantic region. *Int. J. Climatol.* **26**: 233–249, doi: 10.1002/joc.1250.

Shabbar A, Huang JP, Higuchi K. 2001. The relationship between the wintertime North Atlantic Oscillation and blocking episodes in the North Atlantic. *Int. J. Climatol.* **21**: L06125, doi: 10.1002/joc.612.

Smith KL, Kushner PJ. 2012. Linear interference and the initiation of extratropical stratosphere–troposphere interactions. *J. Geophys. Res.* **117**: D13107, doi: 10.1029/2012JD017587.

Strong C, Magnusdottir G. 2008. Tropospheric Rossby wave breaking and the NAO/NAM. *J. Atmos. Sci.* **65**: 2861–2876, doi: 10.1175/2008JAS2632.1.

Taguchi M. 2008. Is there a statistical connection between stratospheric sudden warming and tropospheric blocking events? *J. Atmos. Sci.* **65**: 1442–1454, doi: 10.1175/2007JAS2363.1.

Thompson DWJ, Wallace JM. 1998. The Arctic Oscillation signature in the wintertime geopotential height and temperature fields. *Geophys. Res. Lett.* **25**: 1297–1300, doi: 10.1029/98GL00950.

Thompson DWJ, Baldwin MP, Wallace JM. 2002. Stratospheric connection to Northern Hemisphere wintertime weather: Implications for prediction. *J. Clim.* **15**: 1421–1428, doi: 10.1175/1520-0442(2002)015< 1421:Sctnhw>2.0.Co;2.

Tibaldi S, Molteni F. 1990. On the operational predictability of blocking. *Tellus* **42A**: 343–365, doi: 10.1034/j.1600-0870.1990.t01-2-00003.x.

Vial J, Osborn TJ, Lott F. 2013. Sudden stratospheric warmings and tropospheric blockings in a multi-century simulation of the IPSL-CM5A coupled climate model. *Clim. Dyn.* **40**: 2401–2414, doi: 10.1007/s00382-013-1675-2.

Wang L, Chen W. 2010. Downward Arctic Oscillation signal associated with moderate weak stratospheric polar vortex and the cold December 2009. *Geophys. Res. Lett.* **37**: L09707, doi: 10.1029/2010GL042659.

Woollings T, Charlton-Perez A, Ineson S, Marshall AG, Masato G. 2010. Associations between stratospheric variability and tropospheric blocking. *J. Geophys. Res.* **115**: D06108, doi: 10.1029/2009JD012742.

Xie F, Li JP, Tian WS, Fu Q, Jin FF, Hu YY, Zhang JK, Wang WK, Sun C, Feng J, Yang Y, Ding RQ. 2016. A connection from Arctic stratospheric ozone to El Niño-Southern Oscillation. *Environ. Res. Lett.* **11**: 124026, doi: 10.1088/1748-9326/11/12/124026.

Zhang JK, Tian WS, Chipperfield MP, Xie F, Huang JL. 2016. Persistent shift of the Arctic polar vortex towards the Eurasian continent in recent decades. *Nat. Clim. Change* **6**: 1094–1099, doi: 10.1038/NCLIMATE3136.